

Solution for Flow Rates across the Wellbore in a Two-Zone Confined Aquifer

Shaw-Yang Yang¹ and Hund-Der Yeh²

Abstract: A closed-form solution for transient flow rates across the wellbore in a confined aquifer is derived from a two-zone radial ground-water flow equation subject to the boundary condition of keeping a constant head at the well radius. An aquifer may be considered as a two-zone system if the formation properties near the wellbore are significantly changed due to the well construction and/or well development. An efficient numerical approach is used to evaluate this newly derived solution. Values of the transient flow rate are provided in a tabular form and compared with those obtained by numerical inversion for the Laplace-domain solution. The results show that the two solutions are in good agreement. This newly derived solution can be used not only for predicting the transient flow rate across the wellbore but also for identifying the effects of a skin with a finite thickness on the estimation of transient flow rates in a ground-water system with two different formation properties.

DOI: 10.1061/(ASCE)0733-9429(2002)128:2(175)

CE Database keywords: Flow rates; Ground water; Numerical analysis; Aquifers.

Introduction

The constant-head test is sometimes employed in site characterization for determining the hydraulic parameters of aquifers with low permeability. During the test, the hydraulic head across the wellbore is kept constant while the transient flow rate into the well is measured.

Carslaw and Jaeger (1939) gave the solutions for heat flow from the surface of the region bounded internally by a cylinder such as buried pipe and cable, cooling of mine, etc. Tables of numerical values for the heat-flow rate from the surface which are of practical interest can be seen in Jaeger and Clarke (1942), Ingersoll et al. (1950), and Ingersoll et al. (1954). Based on the solution given by Smith (1937), Jacob and Lohman (1952) presented a formula describing the flow rate across the wellbore in nonleaky confined aquifers and listed a table of the numerical values for a wide range of the dimensionless flow rate versus dimensionless time. Hantush (1962) also provided a formula of ground-water flow through wedge-shaped aquifers, which has the same form as the solution given by Jacob and Lohman (1952). Reed (1980) and Batu (1998) listed a wide range of values of that formula for dimensionless well discharge versus dimensionless distance or time.

During well construction, a wellbore skin of finite thickness may develop due to the invasion of drilling mud into the adjacent formation or the removal of fine particles from the surrounding

formation by extensive well development; consequently, an otherwise homogeneous aquifer may become a two-zone system. The drilling process may therefore produce a positive wellbore skin that has lower hydraulic conductivity than the undisturbed formation. Conversely, thorough well development removes fine particles, e.g., fine silt and clay particles, from the surrounding formation and produces a negative wellbore skin with an increased conductivity. Markle et al. (1995) developed a finite-element model to analyze the transient flow rate across the wellbore during a constant-head test conducted in a vertical fractured media. Their results show that during a constant-head test the transient flow rate across the wellbore may be affected when a wellbore skin exists. Chang and Chen (1999) gave the Laplace-domain solutions of the hydraulic head and the flow rate across the wellbore in a two-zone ground-water system. They presented curves representing specific capacity versus time as part of an investigation of the influence of a skin (low-permeability zone) on aquifer parameter estimations.

In this study a closed-form solution is derived for transient flow rate across the wellbore when performing a constant-head test in a two-zone confined aquifer system. In addition, we present a numerical evaluation of this solution, which is expressed in a dimensionless form. Numerical values of this solution are verified by comparing with the results of numerical inversion for the Laplace-domain solution using the modified Crump algorithm (de Hoog et al. 1982). This new solution can be used as a tool to investigate the effects of the presence of a skin with a finite thickness on the estimation of flow rate across the wellbore.

Mathematical Derivations

Two-Zone Radial Flow Equation under Constant-Head Condition

Fig. 1 shows the well and aquifer configurations for a two-zone confined aquifer system. Several assumptions are made for the solution of hydraulic heads in the confined aquifer; they are (1)

¹Graduate Student, Institute of Environmental Engineering, National Chiao-Tung Univ., Hsinchu, Taiwan.

²Professor, Institute of Environmental Engineering, National Chiao-Tung Univ., Hsinchu, Taiwan.

Note. Discussion open until July 1, 2002. Separate discussions must be submitted for individual papers. To extend the closing date by one month, a written request must be filed with the ASCE Managing Editor. The manuscript for this paper was submitted for review and possible publication on August 18, 2000; approved on July 25, 2001. This paper is part of the *Journal of Hydraulic Engineering*, Vol. 128, No. 2, February 1, 2002. ©ASCE, ISSN 0733-9429/2002/2-175-183/\$8.00+\$0.50 per page.

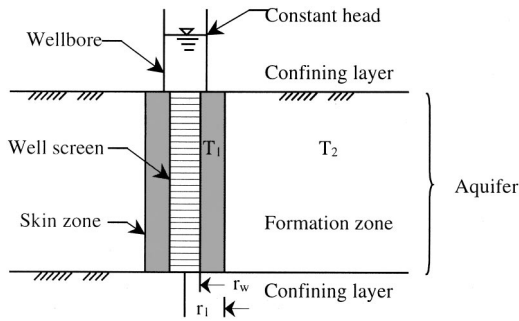


Fig. 1. Schematic diagram of well and aquifer configurations

the aquifer is homogeneous, isotropic, infinite-extent, and with a constant thickness, (2) the well is fully penetrating with a finite radius, and (3) the initial head is constant and uniform throughout the whole aquifer. Based on these assumptions, the governing differential equations in terms of the hydraulic head $h(r,t)$ in two-zone formations can be written as

$$\frac{\partial^2 h_1}{\partial r^2} + \frac{1}{r} \frac{\partial h_1}{\partial r} = \frac{S_1}{T_1} \frac{\partial h_1}{\partial t}, \quad r_w \leq r \leq r_1 \quad (1)$$

and

$$\frac{\partial^2 h_2}{\partial r^2} + \frac{1}{r} \frac{\partial h_2}{\partial r} = \frac{S_2}{T_2} \frac{\partial h_2}{\partial t}, \quad r_1 < r < \infty \quad (2)$$

where the subscripts 1 and 2, respectively, denote the wellbore skin zone and the undisturbed formation zone, h = hydraulic head; r = radial distance from the centerline of the well; r_w = radius of the well; t = time from the start of the test; S = storage coefficient; and T = transmissivity.

The hydraulic head is initially assumed to be zero in both the skin and the undisturbed formation, that is

$$h_1(r,0) = h_2(r,0) = 0, \quad r > r_w \quad (3)$$

The boundary condition for maintaining a constant head at $r = r_w$ is given by

$$h_1(r_w, t) = h_w \quad \text{for } t > 0 \quad (4)$$

where h_w = constant head around the wellbore at any time. As $r \rightarrow \infty$ the hydraulic head tends to zero:

$$h_2(\infty, t) = 0 \quad (5)$$

Between the skin zone and the undisturbed formation the head is continuous

$$h_1(r_1, t) = h_2(r_1, t), \quad t > 0 \quad (6)$$

and there is conservation of mass:

$$T_1 \frac{\partial h_1(r_1, t)}{\partial r} = T_2 \frac{\partial h_2(r_1, t)}{\partial r}, \quad t > 0 \quad (7)$$

Closed-Form Solution

The detailed derivations for the solution of hydraulic head in the Laplace domain for the skin and the undisturbed formation obtained by using Laplace transform for Eqs. (1)–(7) are given in Appendix I and the results for \bar{h}_1 and \bar{h}_2 are respectively expressed as

$$\bar{h}_1 = \frac{h_w}{p} \frac{\phi_1 I_0(q_1 r) - \phi_2 K_0(q_1 r)}{\phi_1 I_0(q_1 r_w) - \phi_2 K_0(q_1 r_w)} \quad (8)$$

and

$$\bar{h}_2 = \frac{h_w}{p} \frac{[\phi_1 I_0(q_1 r_1) - \phi_2 K_0(q_1 r_1)] K_0(q_2 r)}{\phi_1 I_0(q_1 r_w) K_0(q_2 r_1) - \phi_2 K_0(q_1 r_w) K_0(q_2 r_1)} \quad (9)$$

where $q_1^2 = pS_1/T_1$; $q_2^2 = pS_2/T_2$; p = Laplace variable (Spiegel 1965); $I_0(u)$ and $K_0(u)$ = the modified Bessel functions of the first and second kinds of order zero, respectively; and

$$\phi_1 = \sqrt{\frac{S_2 T_2}{S_1 T_1}} K_0(q_1 r_1) K_1(q_2 r_1) - K_1(q_1 r_1) K_0(q_2 r_1) \quad (10)$$

and

$$\phi_2 = \sqrt{\frac{S_2 T_2}{S_1 T_1}} I_0(q_1 r_1) K_1(q_2 r_1) + I_1(q_1 r_1) K_0(q_2 r_1) \quad (11)$$

The functions $I_1(u)$ and $K_1(u)$ are the modified Bessel functions of the first and second kinds of order first, respectively.

Applying Darcy's law at the wellbore, the solution in the Laplace domain for the flow rate across the wellbore \bar{Q}_w can be obtained as

$$\bar{Q}_w = 2\pi r_w T_1 \left\{ \frac{h_w q_1 [\phi_1 I_1(q_1 r_w) + \phi_2 K_1(q_1 r_w)]}{p [\phi_2 K_0(q_1 r_w) - \phi_1 I_0(q_1 r_w)]} \right\} \quad (12)$$

The solution of Eq. (12) in the time domain can be obtained by using the Laplace inversion integral (Hildebrand 1976) as

$$Q_w = 2\pi r_w T_1 \left\{ \frac{2h_w}{\pi} \int_0^\infty e^{-(r_1/S_1)u^2 t} \times \frac{A_1(u)B_2(u) - A_2(u)B_1(u)}{B_1^2(u) + B_2^2(u)} du \right\} \quad (13)$$

with

$$A_1(u) = \sqrt{\frac{S_2 T_2}{S_1 T_1}} [J_0(r_1 u) Y_1(kr_1 u) Y_1(r_w u) - Y_0(r_1 u) Y_1(kr_1 u) J_1(r_w u) - [J_1(r_1 u) Y_0(kr_1 u) Y_1(r_w u) - Y_1(r_1 u) Y_0(kr_1 u) J_1(r_w u)]] \quad (14)$$

$$A_2(u) = \sqrt{\frac{S_2 T_2}{S_1 T_1}} [Y_0(r_1 u) J_1(kr_1 u) J_1(r_w u) - J_0(r_1 u) J_1(kr_1 u) Y_1(r_w u) - [Y_1(r_1 u) J_0(kr_1 u) J_1(r_w u) - J_1(r_1 u) J_0(kr_1 u) Y_1(r_w u)]] \quad (15)$$

$$B_1(u) = \sqrt{\frac{S_2 T_2}{S_1 T_1}} [J_0(r_1 u) Y_1(kr_1 u) Y_0(r_w u) - Y_0(r_1 u) Y_1(kr_1 u) J_0(r_w u) - [J_1(r_1 u) Y_0(kr_1 u) Y_0(r_w u) - Y_1(r_1 u) Y_0(kr_1 u) J_0(r_w u)]] \quad (16)$$

and

$$\begin{aligned}
B_2(u) = & \sqrt{\frac{S_2 T_2}{S_1 T_1}} [Y_0(r_1 u) J_1(k r_1 u) J_0(r_w u) \\
& - J_0(r_1 u) J_1(k r_1 u) Y_0(r_w u)] \\
& - [Y_1(r_1 u) J_0(k r_1 u) J_0(r_w u) \\
& - J_1(r_1 u) J_0(k r_1 u) Y_0(r_w u)] \quad (17)
\end{aligned}$$

where Q_w = flow rate across the wellbore; $k = \sqrt{T_1 S_2 / T_2 S_1}$; $J_0(u)$ and $Y_0(u)$ = the Bessel functions of the first and second kinds of order zero, respectively; and $J_1(u)$ and $Y_1(u)$ = the Bessel functions of the first and second kinds of order first, respectively. Eq. (13) is the closed-form solution to the transient flow rate across the wellbore in a two-zone ground-water system. Detailed derivations to obtain the solution are shown in Appendix II.

Dimensionless Variables

Defining dimensionless variables $\alpha = T_2 / T_1$, $\beta = S_2 / S_1$, $\tau = T_2 t / S_2 r_w^2$, $\rho = r / r_w$, $\rho_1 = r_1 / r_w$, $\bar{Q}_{Dw} = \bar{Q}_w / (2\pi T_2 h_w)$, and $Q_{Dw} = Q_w / (2\pi T_2 h_w)$ where α represents the dimensionless transmissivity, β represents the dimensionless storage coefficient, τ represents the dimensionless time during the test, ρ represents the dimensionless distance from the centerline of the well, ρ_1 represents the dimensionless thickness of the skin, \bar{Q}_{Dw} represents the dimensionless flow rate in the Laplace domain, and Q_{Dw} represents the dimensionless flow rate in the time domain.

The dimensionless flow rate across the wellbore derived from Eq. (12) can be expressed as

$$\bar{Q}_{Dw} = \frac{r_w q_1 [\phi_1 I_1(q_1 r_w) + \phi_2 K_1(q_1 r_w)]}{\alpha p [\phi_2 K_0(q_1 r_w) - \phi_1 I_0(q_1 r_w)]} \quad (18)$$

Accordingly Eq. (13) may be expressed in dimensionless form as

$$Q_{Dw} = \frac{2}{\pi \alpha} \int_0^\infty e^{-\beta \tau u^2 / \alpha} \frac{A'_1(u) B'_2(u) - A'_2(u) B'_1(u)}{B_1'^2(u) + B_2'^2(u)} du \quad (19)$$

where

$$\begin{aligned}
A'_1(u) = & \sqrt{\alpha \beta} [J_0(\rho_1 u) Y_1(k \rho_1 u) Y_1(u) \\
& - Y_0(\rho_1 u) Y_1(k \rho_1 u) J_1(u)] - [J_1(\rho_1 u) Y_0(k \rho_1 u) Y_1(u) \\
& - Y_1(\rho_1 u) Y_0(k \rho_1 u) J_1(u)] \quad (20)
\end{aligned}$$

$$\begin{aligned}
A'_2(u) = & \sqrt{\alpha \beta} [Y_0(\rho_1 u) J_1(k \rho_1 u) J_1(u) \\
& - J_0(\rho_1 u) J_1(k \rho_1 u) Y_1(u)] - [Y_1(\rho_1 u) J_0(k \rho_1 u) J_1(u) \\
& - J_1(\rho_1 u) J_0(k \rho_1 u) Y_1(u)] \quad (21)
\end{aligned}$$

$$\begin{aligned}
B'_1(u) = & \sqrt{\alpha \beta} [J_0(\rho_1 u) Y_1(k \rho_1 u) Y_0(u) \\
& - Y_0(\rho_1 u) Y_1(k \rho_1 u) J_0(u)] - [J_1(\rho_1 u) Y_0(k \rho_1 u) Y_0(u) \\
& - Y_1(\rho_1 u) Y_0(k \rho_1 u) J_0(u)] \quad (22)
\end{aligned}$$

and

$$\begin{aligned}
B'_2(u) = & \sqrt{\alpha \beta} [Y_0(\rho_1 u) J_1(k \rho_1 u) J_0(u) \\
& - J_0(\rho_1 u) J_1(k \rho_1 u) Y_0(u)] - [Y_1(\rho_1 u) J_0(k \rho_1 u) J_0(u) \\
& - J_1(\rho_1 u) J_0(k \rho_1 u) Y_0(u)] \quad (23)
\end{aligned}$$

If the aquifer properties are assumed to be constant through the

whole aquifer, then Eq. (19), the flow rate across the wellbore in the dimensionless form, can be reduced to the single-zone solution presented by Jaeger and Clarke (1942) as

$$\frac{Q_w}{2\pi T_2 h_w} = \frac{4}{\pi^2} \int_0^\infty \frac{e^{-\tau u^2}}{[J_0^2(u) + Y_0^2(u)] u} du \quad (24)$$

Numerical Evaluation

Bessel Functions

Eq. (18) includes the Bessel functions $I_0(u)$, $I_1(u)$, $K_0(u)$, and $K_1(u)$. Likewise, Eq. (19) contains the integral composing of $J_0(u)$, $J_1(u)$, $Y_0(u)$, and $Y_1(u)$. These functions approximated by the formulas given in Abramowitz and Stegun (1964) and Watson (1958) are listed in Appendix III. The argument u in these formulas may be divided into two ranges, $[0,10]$ and $(10,\infty)$ for $I_0(u)$ and $I_1(u)$, $[0,2]$ and $(2,\infty)$ for $K_0(u)$ and $K_1(u)$, and $[0,12]$ and $(12,\infty)$ for $J_0(u)$, $J_1(u)$, $Y_0(u)$, and $Y_1(u)$ in order to achieve better accuracy. Besides, these formulas are essentially composed of infinite series and may converge slowly, especially when u is small. Therefore, the Shanks method (Shanks 1955; Wynn 1956) is employed to accelerate the convergence when evaluating the series. Each function in the integrands of Eqs. (18) and (19) is calculated to ten decimal places, and thus it bears the same degree of accuracy as those listed in Abramowitz and Stegun (1964).

Shanks Method

The Shanks transform, also called the ϵ algorithm, consists of a family of nonlinear sequence-to-sequence transformations (Shanks 1955). Shanks (1955) proved that these transformations are effective when applied to accelerate the convergence of some slowly convergent sequences and may converge some divergent sequences. Examples of the applications of Shanks method include numerical series, the power series of rational and meromorphic functions, and a wide variety of sequences drawn from integral equations, geometry, fluid mechanics, and number theory (Shanks 1955).

The partial sums, S_n , of an infinite series may be denoted as

$$S_n = \sum_{k=1}^n a_k \quad (25)$$

where a_k is the k th term of the series. Based on the sequence of partial sums, the Shanks transform may be expressed as (Wynn 1956)

$$e_{i+1}(S_n) = e_{i-1}(S_{n+1}) + \frac{1}{e_i(S_{n+1}) - e_i(S_n)}, \quad i = 1, 2, \dots \quad (26)$$

where $e_0(S_n) = S_n$ and $e_1(S_n) = [e_0(S_{n+1}) - e_0(S_n)]^{-1}$.

It is necessary to set a certain convergence criterion when applying the Shanks transform to evaluate a given series. Therefore, one may define a convergence factor, ERR, as

$$|e_{2i+2}(S_{n-1}) - e_{2i}(S_n)| \leq \text{ERR} \quad (27)$$

The sequence of partial sums is terminated when this criterion is met and the infinite series converges to the estimated value of $e_{2i+2}(S_{n-1})$.

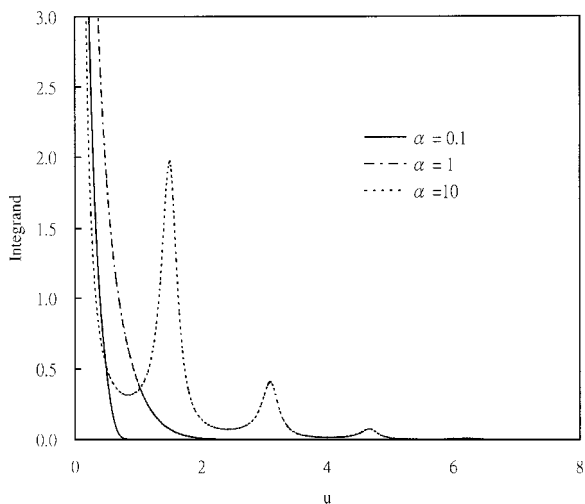


Fig. 2. Plot of integrand of Eq. (19) versus u for $\rho=1$, $\rho_1=3$, $\beta=1$, and $\tau=1$ while $\alpha=0.1, 1$, or 10

Numerical Inversion

In many engineering problems, the Laplace-domain solutions for mathematical models are tractable, yet the corresponding solutions in the time domain may not be entirely possible or easily solved. Under such circumstances, a numerical inversion such as the Stehfest algorithm (Stehfest 1970) or the Crump algorithm (Crump 1976) may be used. Eq. (18) is numerically inverted by using the modified Crump algorithm (de Hoog et al. 1982), which is based on the ε -algorithm to evaluate the corresponding diagonal Pade approximants (IMSL 1987).

Gaussian Quadrature

Gaussian quadrature is widely used in performing the numerical integration of a known function. The integration limits of $\int_a^b f(x) dx$ are changed from $[a, b]$ to $[-1, 1]$ by a suitable transformation of variable when applying Gaussian quadrature. The formula for an n -point Gaussian quadrature may be written as (Gerald and Wheatley 1989)

$$\int_{-1}^1 f(\xi) d\xi = \sum_{i=1}^n W_i f(\xi_i) \quad (28)$$

where W_i = weighting factor and ξ_i = integration point. Values for W_i and ξ_i can be found in books on the fields of numerical methods (e.g., Burden and Faires 1989; Gerald and Wheatley 1989) and the fields of finite element methods (e.g., Reddy 1984; Burnett 1987).

Integration Procedures for the Closed-Form Solution

Fig. 2 demonstrates the plots of the integrand of Eq. (19) versus u for $\rho=1$, $\rho_1=3$, $\beta=1$, and $\tau=1$ while $\alpha=0.1, 1$, or 10 . The two-zone aquifer becomes a homogenous (single zone) aquifer system when $\alpha=1$; on the other hand, the aquifer has a negative skin when $\alpha=0.1$ and a positive skin when $\alpha=10$. It can be observed that the integrand of Eq. (19) approaches infinity as u tends to 0; contrarily, the integrand tends to zero as u becomes very large.

The closed-form solution for the dimensionless flow rate, Eq. (19), cannot be directly evaluated because the integrand contains a singular point at the origin as indicated in Fig. 2. Letting ε to be

a very small value, say 10^{-20} , and starting from ε , Eq. (19) can be evaluated by Gaussian quadrature. The initial interval for numerical integration in Eq. (19) is chosen as 10^{-5} ; then, both six-point and ten-point formulas of Gaussian quadrature are used at the same time to carry out the integration of Eq. (19). If the difference of the results by those two formulas is less than the prescribed criterion, say 10^{-7} , a double interval will be used for next integration. Otherwise, the present interval will be divided into two equal portions, and the same approach is again applied to each portion until the result for each portion is less than 10^{-7} . This procedure ensures that each result has the accuracy to seven decimal places. The same integration procedures are applied to succeeding integrations until the difference in the result for each portion is less than 10^{-7} . Then the remaining integration is obtained by changing the variable as $y=1/u$ and the transformed integral in terms of y is directly evaluated by Gaussian quadrature (Gerald and Wheatley 1989, p. 304). Therefore, the result of numerical integrations for the flow rate can be obtained by simply adding all the results from each interval or portion.

Results

Comparisons between the closed-form solution of Eq. (19) and the results obtained from numerical inversion of Eq. (18) may provide a cross check for the validity and accuracy of both solutions. The values of dimensionless flow rate versus dimensionless time from 0.01 to 1000 evaluated by the proposed numerical approach for Eq. (19) and the modified Crump algorithm for Eq. (18) are listed in Tables 1 and 2, respectively, for single-zone and two-zone systems. Table 1 gives the values of dimensionless flow rate versus dimensionless time for $\rho_1=3$ and $\beta=1$ when $\alpha=1$, that is, when the aquifer formation is under the single-zone condition. An approach of infinite series expansion given in Harvard's problem report (1950) is adopted to remove the singularity of the integrand of Eq. (24) when performing the integration from zero to ε . For the integration limit from ε to infinity, Eq. (24) is evaluated by previously suggested integration procedures. The flow rates estimated by the numerical inversion for the Laplace-domain solution and those given in Jaeger and Clarke (1942) agree to three decimal places when compared to that of the closed-form solution as shown in Table 1. Table 2 shows the plot of the dimensionless flow rate versus dimensionless time for $\rho_1=3$ and $\beta=1$ when $\alpha=0.1$ or 10 . The formation has a negative skin when $\alpha=0.1$ and a positive skin when $\alpha=10$. The flow rate values obtained by numerical Laplace inversion agree well with that of the closed-form solution. This indicates that this closed-form solution yields accurate results for the presence of a wellbore skin when estimated by the proposed numerical approach. Fig. 3 shows that the curve representing the dimensionless flow rate across the wellbore for the undisturbed (single-zone) formation is quite different from that with positive or negative wellbore skin. If a positive wellbore skin exists, then the dimensionless flow rate is smaller than that when a negative wellbore skin exists at the same dimensionless time. A smaller flow rate across the wellbore reflects the result of lower hydraulic conductivity of the positive skin. Conversely, a larger dimensionless flow rate is considered to reflect the increase of formation conductivity and storage effects in the presence of a negative wellbore skin.

Conclusions

A closed-form solution for describing the transient flow rate across the wellbore in a two-zone confined ground-water system

Table 1. Dimensionless Flow Rate versus Dimensionless Time (τ) Estimated by Closed-Form Solution, Numerical Inversion from Laplace-Domain Solution, and One Given in Jaeger and Clarke (1942) for $\rho_1=3$ and $\beta=1$ when $\alpha=1$

τ	Closed-form		Jaeger and Clarke
	solution	Numerical inversion solution	
0.01	6.127	6.129	6.219
0.02	4.470	4.472	4.472
0.03	3.735	3.736	3.736
0.04	3.295	3.297	3.297
0.05	2.995	2.997	2.997
0.06	2.773	2.774	2.775
0.07	2.600	2.601	2.602
0.08	2.461	2.462	2.463
0.09	2.345	2.346	2.347
0.1	2.247	2.248	2.249
0.2	1.714	1.715	1.715
0.3	1.475	1.476	1.476
0.4	1.331	1.332	1.333
0.5	1.232	1.233	1.234
0.6	1.159	1.160	1.160
0.7	1.101	1.102	1.102
0.8	1.054	1.056	1.056
0.9	1.015	1.017	1.017
1	0.982	0.984	0.984
2	0.799	0.800	0.800
3	0.715	0.716	0.716
4	0.663	0.664	0.664
5	0.627	0.628	0.628
6	0.599	0.601	0.601
7	0.578	0.579	0.579
8	0.560	0.561	0.562
9	0.545	0.547	0.547
10	0.532	0.534	0.534
20	0.460	0.461	0.461
30	0.425	0.426	0.426
40	0.403	0.404	0.404
50	0.387	0.388	0.388
60	0.375	0.376	0.376
70	0.365	0.366	0.366
80	0.357	0.358	0.358
90	0.350	0.351	0.352
100	0.344	0.346	0.346
200	0.309	0.311	0.311
300	0.292	0.293	0.294
400	0.281	0.282	0.282
500	0.272	0.274	0.274
600	0.266	0.267	0.268
700	0.261	0.262	0.263
800	0.256	0.258	0.258
900	0.253	0.254	0.255
1000	0.246	0.251	0.251

Table 2. Dimensionless Flow Rate versus Dimensionless Time τ Estimated by Closed-Form Solution (CS) and Numerical Inversion Solution (NS) for $\rho_1=3$ and $\beta=1$ when $\alpha=0.1$ or 10

τ	$\alpha=0.1$		$\alpha=10$	
	(negative skin)		(positive skin)	
	CS	NS	CS	NS
0.01	22.479	22.488	1.830	1.833
0.02	17.144	17.152	1.307	1.311
0.03	14.754	14.763	1.075	1.079
0.04	13.316	13.324	0.937	0.941
0.05	12.324	12.333	0.843	0.847
0.06	11.581	11.592	0.773	0.777
0.07	10.990	11.003	0.719	0.723
0.08	10.497	10.513	0.676	0.679
0.09	10.073	10.090	0.639	0.643
0.1	9.698	9.713	0.609	0.613
0.2	7.198	7.080	0.443	0.447
0.3	5.726	5.480	0.370	0.374
0.4	4.749	4.443	0.326	0.330
0.5	4.066	3.739	0.296	0.300
0.6	3.569	3.241	0.273	0.277
0.7	3.195	2.877	0.256	0.260
0.8	2.908	2.603	0.242	0.246
0.9	2.681	2.391	0.231	0.235
1	2.498	2.225	0.221	0.225
2	1.675	1.515	0.167	0.171
3	1.390	1.282	0.144	0.148
4	1.236	1.156	0.129	0.133
5	1.135	1.073	0.119	0.123
6	1.063	1.012	0.112	0.116
7	1.008	0.965	0.106	0.110
8	0.963	0.927	0.102	0.106
9	0.927	0.895	0.099	0.102
10	0.896	0.868	0.096	0.100
20	0.728	0.718	0.083	0.089
30	0.653	0.649	0.080	0.087
40	0.606	0.605	0.079	0.086
50	0.574	0.575	0.078	0.085
60	0.550	0.552	0.077	0.084
70	0.530	0.533	0.077	0.083
80	0.515	0.518	0.076	0.083
90	0.501	0.505	0.076	0.082
100	0.490	0.494	0.075	0.082
200	0.425	0.431	0.073	0.079
300	0.393	0.400	0.072	0.077
400	0.373	0.380	0.071	0.076
500	0.359	0.366	0.070	0.075
600	0.348	0.355	0.070	0.075
700	0.339	0.347	0.069	0.074
800	0.332	0.340	0.069	0.074
900	0.326	0.333	0.069	0.074
1000	0.320	0.328	0.069	0.073

has been developed for the constant-head test with the presence of a wellborn skin. This solution was derived using Laplace transform and a contour integral method. In a single-zone aquifer system, the transient dimensionless flow rates computed from the closed-form solution match well with those given by Jaeger and Clarke (1942) and the Laplace-domain solution. Under the two-zone condition, i.e., in the presence of a positive or negative

wellbore skin, the results of the closed-form solution agree with those of the Laplace-domain solution to two decimal places. This provides a double check for the correctness of the closed-form solution.

The flow rate decreases rapidly with increasing time at the early stage of the test and asymptotically approaches a constant value for a long test period. For small times the differences be-

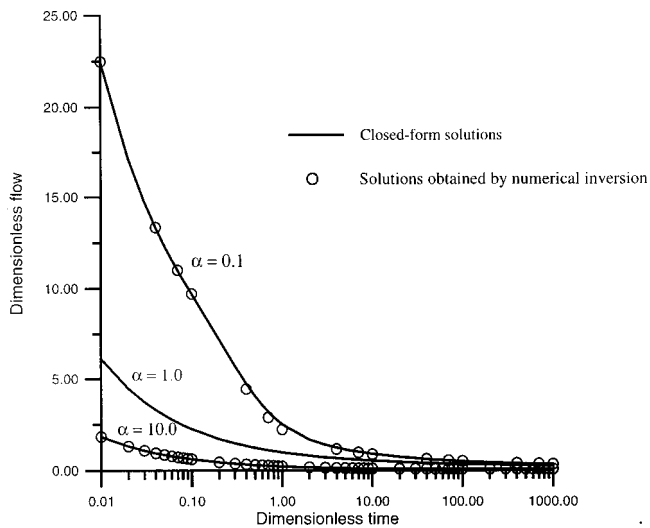


Fig. 3. Results of the closed-form solution evaluated by the numerical approach and the solution obtained from the numerical inversion by using the modified crump approach.

tween the flow rate in an aquifer with a positive or negative wellbore skin and an aquifer without a wellbore skin are large. In addition, the effect of a negative wellbore skin on the flow rate is larger than that of a positive wellbore skin. Obviously, the magnitude of the flow rate across the wellbore strongly depends on the hydraulic properties of both the formation and the wellbore skin.

Acknowledgments

The writers appreciate the comments and suggested revisions of two anonymous reviewers that help improve the clarity of our presentation. Research leading to this paper has been partly supported by the grants from Taiwan Power Company via National Science Council of ROC under Contract No. NSC89-TPC-E-099-001.

Appendix I. Derivation of Eqs. (8) and (9)

Chang and Chen (1999) presented the Laplace-domain solutions of the hydraulic head and the flow rate across the wellbore in a two-zone ground-water system without giving the derivations. Nevertheless, such solutions in the Laplace domain, Eqs. (8) and (9), can be derived based on the procedures given in Carslaw and Jaeger (1959).

Applying the Laplace transform on Eqs. (1) and (2) yields

$$\frac{d^2 \bar{h}_1}{dr^2} + \frac{1}{r} \frac{d\bar{h}_1}{dr} = q_1^2 \bar{h}_1 \quad (29)$$

and

$$\frac{d^2 \bar{h}_2}{dr^2} + \frac{1}{r} \frac{d\bar{h}_2}{dr} = q_2^2 \bar{h}_2 \quad (30)$$

Furthermore, Laplace transforms of boundary conditions, Eqs. (4)–(7), are

$$\bar{h}_1 = h_w / p \quad \text{for } r = r_w \quad (31)$$

$$\bar{h}_2 = 0 \quad \text{for } r \rightarrow \infty \quad (32)$$

$$\bar{h}_1 = \bar{h}_2 \quad \text{for } r = r_1 \quad (33)$$

and

$$T_1 \frac{d\bar{h}_1}{dr} = T_2 \frac{d\bar{h}_2}{dr} \quad \text{for } r = r_1 \quad (34)$$

The solutions of Eqs. (8) and (9) to the hydraulic head in the Laplace domain in the skin and the undisturbed formation can then be obtained as (Carslaw and Jaeger 1959)

$$\bar{h}_1 = C_1 I_0(q_1 r) + C_2 K_0(q_1 r) \quad (35)$$

and

$$\bar{h}_2 = D_1 I_0(q_2 r) + D_2 K_0(q_2 r) \quad (36)$$

where C_1 , C_2 , D_1 , and D_2 are constants.

Substituting Eqs. (35) and (36) into Eqs. (31)–(34), one can obtain

$$C_1 = \frac{h_w}{p} \frac{\phi_1}{\phi_1 I_0(q_1 r_w) - \phi_2 K_0(q_1 r_w)} \quad (37)$$

$$C_2 = \frac{h_w}{p} \frac{-\phi_2}{\phi_1 I_0(q_1 r_w) - \phi_2 K_0(q_1 r_w)} \quad (38)$$

$$D_1 = 0 \quad (39)$$

and

$$D_2 = \frac{h_w}{p} \frac{\phi_1 I_0(q_1 r_1) - \phi_2 K_0(q_1 r_1)}{\phi_1 I_0(q_1 r_w) K_0(q_2 r_1) - \phi_2 K_0(q_1 r_w) K_0(q_2 r_1)} \quad (40)$$

Consequently, Eq. (8) can be obtained by substituting the constants from Eqs. (37) and (38) into Eqs. (35) and (9) can be obtained by a similar manner. Note that Eq. (9), representing the head distribution in the undisturbed formation, slightly differs from the one given in Chang and Chen (1999). Their inaccuracy may be due to typing errors.

Appendix II. Derivation of Eq. (13)

The inverse Laplace transform of Eq. (12) in the time domain can be obtained by using the Laplace inversion integral (Hildebrand 1976) as

$$Q_w = \frac{1}{2\pi i} \int_{\zeta - i\infty}^{\zeta + i\infty} e^{pt} \bar{Q}_w dp \quad (41)$$

where p = complex variable; i = imaginary unit; and ζ = large, real, positive constant, so much so that all the poles lie to the left of the line ($\zeta - i\infty, \zeta + i\infty$).

A single branch point with no singularity (pole) at $p=0$ exists in the integrand of Eq. (12). Thus, this integration may require the use of the Bromwich integral for the Laplace inversion. The closed contour of the integrand is shown in Fig. 4 with a cut of the p plane along the negative real axis, where δ is taken sufficiently small to exclude all poles from the circle about the origin.

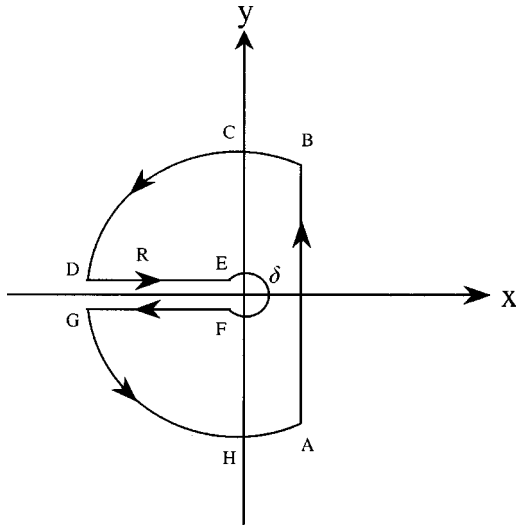


Fig. 4. Plot of closed contour integration of \bar{h} for inverse Laplace transform (Hildebrand 1976)

The closed contour consists of the part AB of the Bromwich line from $-\infty$ to ∞ , semicircles BCD and GHA , lines DE and FG parallel to the real axis and a circle EF of radius δ about the origin. The integration along the small circle EF around the origin as $\delta \rightarrow 0$ is carried out by using the Cauchy integral and the value of the integration is equal to zero. The integrals taken along BCD and GHA tend to zero as $R \rightarrow \infty$. Consequently, Eq. (12) can be superseded by the sum of the integrals along DE and FG . In other words, the integral can then be written as

$$Q_w = \lim_{\substack{\delta \rightarrow 0 \\ R \rightarrow \infty}} \frac{1}{2\pi i} \left[\int_{DE} e^{pt} \bar{Q}_w dp + \int_{FG} e^{pt} \bar{Q}_w dp \right] \quad (42)$$

For the first term on the right-hand side (RHS) of Eq. (42) along DE we introduce the change of variable $p = u^2 e^{-\pi i} T_1 / S_1$ and use the formula (Carslaw and Jaeger 1959, p. 490)

$$K_\nu(z e^{\pm(1/2)\pi i}) = \pm \frac{1}{2} \pi i e^{\mp(1/2)v\pi i} [-J_\nu(z) \pm i Y_\nu(z)] \quad (43)$$

and

$$I_\nu(z e^{\pm(1/2)\pi i}) = e^{\pm(1/2)v\pi i} J_\nu(z) \quad (44)$$

where $\nu = 0, 1, 2, \dots$. The first term on the RHS of Eq. (42) then leads to

$$Q_{w1} = -\frac{2r_w T_1 h_w}{i} \int_0^\infty -e^{(T_1/S_1)u^2 t} \frac{[A_1(u) + iA_2(u)]}{[B_1(u) + iB_2(u)]} du \quad (45)$$

Likewise, introducing $p = u^2 e^{\pi i} T_1 / S_1$, the integral along EF gives minus the conjugate of Eq. (45) as

$$Q_{w2} = \frac{2r_w T_1 h_w}{i} \int_0^\infty -e^{(T_1/S_1)u^2 t} \frac{[A_1(u) - iA_2(u)]}{[B_1(u) - iB_2(u)]} du \quad (46)$$

The closed-form solution of Eq. (13) can then be obtained by combining Eqs. (45) and (46).

Appendix III. Formulas of Bessel Functions

The Bessel functions of $I_0(u)$, $I_1(u)$, $K_0(u)$, and $K_1(u)$ may be evaluated by the formulas given in Abramowitz and Stegun (1964). The argument u in these formulas can be divided into two ranges, $[0, 10]$ and $(10, \infty)$ for $I_0(u)$ and $I_1(u)$ and $[0, 2]$ and $(2, \infty)$ for $K_0(u)$ and $K_1(u)$ for better accuracy. For $0 \leq u \leq 10$, the asymptotic expansions for $I_0(u)$ and $I_1(u)$ may be expressed respectively as (Abramowitz and Stegun 1964, p. 375)

$$I_0(u) = 1 + \frac{1}{4}u^2 + \frac{\left(\frac{1}{4}u^2\right)^2}{(1!)^2} + \frac{\left(\frac{1}{4}u^2\right)^3}{(2!)^2} + \dots \quad (47)$$

and

$$I_1(u) = \left(\frac{u}{2}\right) \left[1 + \frac{\frac{1}{4}u^2}{(1!)(2!)} + \frac{\left(\frac{1}{4}u^2\right)^2}{(2!)(3!)} + \frac{\left(\frac{1}{4}u^2\right)^3}{(3!)(4!)} + \dots \right] \quad (48)$$

The Bessel functions of $I_0(u)$ and $I_1(u)$ for $10 < u < \infty$ are respectively approximated as (Abramowitz and Stegun 1964, p. 377)

$$I_0(u) = \frac{e^u}{\sqrt{2\pi u}} \left\{ 1 + \frac{1^2}{(1!)(8u)} + \frac{1^2 \times 3^2}{(2!)(8u)^2} + \frac{1^2 \times 3^2 \times 5^2}{(3!)(8u)^3} + \dots \right\} \quad (49)$$

and

$$I_1(u) = \frac{e^u}{\sqrt{2\pi u}} \left\{ 1 - \frac{4-1^2}{(1!)(8u)} + \frac{(4-1^2) \cdot (4-3^2)}{(2!)(8u)^2} - \frac{(4-1^2) \cdot (4-3^2) \cdot (4-5^2)}{(3!)(8u)^3} + \dots \right\} \quad (50)$$

For $0 \leq u \leq 2$, the asymptotic expansions for $K_0(u)$ and $K_1(u)$ may be written respectively as (Abramowitz and Stegun 1964, p. 375)

$$K_0(u) = -\left[\ln\left(\frac{u}{2}\right) + \gamma \right] I_0(u) + \frac{1}{(1!)^2} + \left(1 + \frac{1}{2}\right) \frac{\left(\frac{1}{4}u^2\right)^2}{(2!)^2} + \left(1 + \frac{1}{2} + \frac{1}{3}\right) \frac{\left(\frac{1}{4}u^2\right)^3}{(3!)^2} + \dots \quad (51)$$

and

$$K_1(u) = \left[\ln\left(\frac{u}{2}\right) + \gamma \right] I_1(u) + \frac{1}{u} - \frac{u}{4} \left\{ \begin{aligned} & \left[\frac{\frac{1}{4}u^2}{(1!)(2!)} + \left(1 + \frac{1}{2}\right) \frac{\left(\frac{1}{4}u^2\right)^2}{(2!)(3!)} + \left(1 + \frac{1}{2} + \frac{1}{3}\right) \frac{\left(\frac{1}{4}u^2\right)^3}{(3!)(4!)} + \dots \right] \\ & + \left[1 + \left(1 + \frac{1}{2}\right) \frac{\frac{1}{4}u^2}{(1!)(2!)} + \left(1 + \frac{1}{2} + \frac{1}{3}\right) \frac{\left(\frac{1}{4}u^2\right)^2}{(2!)(3!)} + \dots \right] \end{aligned} \right\} \quad (52)$$

where $\gamma = 0.577215664901533$ is the Euler's constant. For $2 < u < \infty$, $K_0(u)$ and $K_1(u)$ are respectively taken as (Abramowitz and Stegun 1964, p. 378)

$$K_0(u) = \frac{e^u}{\sqrt{2\pi u}} \left\{ 1 - \frac{1^2}{(1!)(8u)} + \frac{1^2 \times 3^2}{(2!)(8u)^2} - \frac{1^2 \times 3^2 \times 5^2}{(3!)(8u)^3} + \dots \right\} \quad (53)$$

and

$$K_1(u) = \frac{e^u}{\sqrt{2\pi u}} \left\{ 1 + \frac{4-1^2}{(1!)(8u)} + \frac{(4-1^2) \cdot (4-3^2)}{(2!)(8u)^2} + \frac{(4-1^2) \cdot (4-3^2) \cdot (4-5^2)}{(3!)(8u)^3} + \dots \right\} \quad (54)$$

These functions of $J_0(u)$, $J_1(u)$, $Y_0(u)$, and $Y_1(u)$ may be evaluated by the formulas given in Abramowitz and Stegun (1964) and Watson (1958). The argument u in these four functions may be split into two ranges, $[0, 12]$ and $(12, \infty)$, for good accuracy. For $0 \leq u \leq 12$, these functions may be written respectively as (Abramowitz and Stegun 1964, p. 360)

$$J_0(u) = 1 - \frac{\frac{1}{4}u^2}{(1!)^2} + \frac{\left(\frac{1}{4}u^2\right)^2}{(2!)^2} - \frac{\left(\frac{1}{4}u^2\right)^3}{(3!)^2} + \dots \quad (55)$$

$$J_1(u) = \left(\frac{u}{2}\right) \left[1 - \frac{\frac{1}{4}u^2}{(1!)(2!)} + \frac{\left(\frac{1}{4}u^2\right)^2}{(2!)(3!)} - \frac{\left(\frac{1}{4}u^2\right)^3}{(3!)(4!)} + \dots \right] \quad (56)$$

$$Y_0(u) = \frac{2}{\pi} \left[\ln\left(\frac{u}{2}\right) + \gamma \right] J_0(u) + \frac{2}{\pi} \left[\frac{\frac{1}{4}u^2}{(1!)^2} - \left(1 + \frac{1}{2}\right) \frac{\left(\frac{1}{4}u^2\right)^2}{(2!)^2} + \left(1 + \frac{1}{2} + \frac{1}{3}\right) \frac{\left(\frac{1}{4}u^2\right)^3}{(3!)^2} - \dots \right] \quad (57)$$

and

$$Y_1(u) = -\frac{2}{\pi u} + \frac{2}{\pi} \left[\ln\left(\frac{u}{2}\right) + \gamma \right] J_1(u) + \frac{u}{2\pi} \left\{ \begin{aligned} & \left[-\frac{\frac{1}{4}u^2}{(1!)(2!)} + \left(1 + \frac{1}{2}\right) \frac{\left(\frac{1}{4}u^2\right)^2}{(2!)(3!)} - \left(1 + \frac{1}{2} + \frac{1}{3}\right) \frac{\left(\frac{1}{4}u^2\right)^3}{(3!)(4!)} + \dots \right] \\ & + \left[1 - \left(1 + \frac{1}{2}\right) \frac{\frac{1}{4}u^2}{(1!)(2!)} + \left(1 + \frac{1}{2} + \frac{1}{3}\right) \frac{\left(\frac{1}{4}u^2\right)^2}{(2!)(3!)} - \dots \right] \end{aligned} \right\} \quad (58)$$

Note that as $u=0$, $J_0(u)$ and $J_1(u)$ are equal to one and zero respectively, whereas $Y_0(u)$ and $Y_1(u)$ approach $-\infty$.

The functions of $J_0(u)$, $J_1(u)$, $Y_0(u)$, and $Y_1(u)$ for $12 < u < \infty$ are approximated respectively as (Watson 1958, p. 199)

$$J_0(u) = \sqrt{\frac{2}{\pi u}} \left\{ \cos\left(u - \frac{\pi}{4}\right) \left[\sum_{m=0}^{\infty} \frac{(-1)^m \cdot (0, 2m)}{(2u)^{2m}} \right] - \sin\left(u - \frac{\pi}{4}\right) \left[\sum_{m=0}^{\infty} \frac{(-1)^m \cdot (0, 2m+1)}{(2u)^{2m+1}} \right] \right\} \quad (59)$$

$$J_1(u) = \sqrt{\frac{2}{\pi u}} \left\{ \cos\left(u - \frac{3\pi}{4}\right) \left[\sum_{m=0}^{\infty} \frac{(-1)^m \cdot (1, 2m)}{(2u)^{2m}} \right] - \sin\left(u - \frac{3\pi}{4}\right) \left[\sum_{m=0}^{\infty} \frac{(-1)^m \cdot (1, 2m+1)}{(2u)^{2m+1}} \right] \right\} \quad (60)$$

$$Y_0(u) = \sqrt{\frac{2}{\pi u}} \left\{ \sin\left(u - \frac{\pi}{4}\right) \left[\sum_{m=0}^{\infty} \frac{(-1)^m \cdot (0, 2m)}{(2u)^{2m}} \right] + \cos\left(u - \frac{\pi}{4}\right) \left[\sum_{m=0}^{\infty} \frac{(-1)^m \cdot (0, 2m+1)}{(2u)^{2m+1}} \right] \right\} \quad (61)$$

and

$$Y_1(u) = \sqrt{\frac{2}{\pi u}} \left\{ \sin\left(u - \frac{3\pi}{4}\right) \left[\sum_{m=0}^{\infty} \frac{(-1)^m \cdot (1, 2m)}{(2u)^{2m}} \right] + \cos\left(u - \frac{3\pi}{4}\right) \left[\sum_{m=0}^{\infty} \frac{(-1)^m \cdot (1, 2m+1)}{(2u)^{2m+1}} \right] \right\} \quad (62)$$

where

$$(v, m) = \frac{\Gamma\left(v + m + \frac{1}{2}\right)}{m! \Gamma\left(v - m + \frac{1}{2}\right)} \quad (63)$$

and $\Gamma(m)$ is the Gamma function (Abramowitz and Stegun 1964, p. 255).

References

- Abramowitz, M., and Stegun, I. A. (1964). *Handbook of mathematical functions with formulas, graphs and mathematical tables*, National Bureau of Standards, Dover, Washington, D.C.
- Batu, V. (1998). *Aquifer hydraulics: A comprehensive guide to hydrogeologic data analysis*, Wiley, New York.
- Burden, R. L., and Faires, J. D. (1989). *Numerical analysis*, 4th Ed., PWS-KENT, Boston.
- Burnett, D. S. (1987). *Finite element analysis*, Addison-Wesley, Redwood City, Calif.
- Carslaw, H. S., and Jaeger, J. C. (1939). "Some two-dimensional problems in conduction of heat with circular symmetry." *Some Problems in Conduction of Heat*, 46, 361–388.
- Carslaw, H. S., and Jaeger, J. C. (1959). *Conduction of heat in solids*, 2nd Ed., Clarendon, Oxford.
- Chang, C. C., and Chen, C. S. (1999). "Analysis of constant-head for a two-zone radially symmetric nonuniform model." *Proc. 3rd Ground-water Resources and Water Quality Protection Conf.*, National Central Univ., Chung-Li, Taiwan.
- Crump, K. S. (1976). "Numerical inversion of Laplace transforms using a Fourier series approximation." *J. Assoc. Comput. Mach.*, 23(1), 89–96.
- de Hoog, F. R., Knight, J. H., and Stokes, A. N. (1982). "An improved method for numerical inversion of Laplace transforms." *Soc. Industrial Appl. Mathe. J. Sci. Stat. Comput.*, 3(3), 357–366.
- Gerald, C. F., and Wheatley, P. O. (1989). *Applied numerical analysis*, 4th Ed., Addison-Wesley, Reading, Mass.
- Hantush, M. S. (1962). "Flow of ground water in sands of nonuniform thickness; Part 1. Flow in a wedge-shaped aquifer." *J. Geophys. Res.*, 67(2), 703–709.
- Harvard Problem Report (1950). "A function describing the conduction of heat in a solid medium bounded internally by a cylindrical surface," Computation Laboratory of Harvard Univ. *Rep. No. 76*.
- Hildebrand, F. B. (1976). *Advanced calculus for applications*, 2nd Ed., Prentice-Hall, Englewood Cliffs, N.J.
- Ingersoll, L. R., Adler, F. T. W., Plass, H. J., and Ingersoll, A. G. (1950). "Theory of earth heat exchangers for the heat pump." *Heat/Piping/Air Cond.*, 113–122.
- Ingersoll, L. R., Zobel, O. J., and Ingersoll, A. C. (1954). *Heat conduction with engineering, geological, and other applications*, 2nd Ed., University Wisconsin Press, Madison, Wis.
- International Mathematics and Statistics Library, Inc. (1987). *IMSL User's Manual*, 2, IMSL, Inc., Houston.
- Jacob, C. E., and Lohman, S. W. (1952). "Nonsteady flow to a well of constant drawdown in an extensive aquifer." *Trans., Am. Geophys. Union*, 33(4), 559–569.
- Jaeger, J. C., and Clarke, M. (1942). "A short table of $I_0(i; x)$." *Proc. R. Soc. Edinburgh, Sect. A: Math. Phys. Sci.*, 61, 229–230.
- Markle, J. M., Rowe, R. K., and Novakowski, K. S. (1995). "A model for the constant-heat pumping test conducted in vertically fractured media." *Int. J. Numer. Analyt. Meth. Geomech.*, 19, 457–473.
- Reddy, J. N. (1984). *An introduction to the finite element method*, McGraw-Hill, New York.
- Reed, J. E. (1980). *Type curves for selected problems of flow to wells in confined aquifers; Book 3 applications of hydraulics*, United States Department of the Interior, US GPO, Washington, D.C.
- Shanks, D. (1955). "Non-linear transformations of divergent and slowly convergent sequences." *J. Math. Phys.*, 34, 1–42.
- Smith, L. P. (1937). "Heat flow in an infinite solid bounded internally by a cylinder." *J. Appl. Phys.*, 8(6), 45–49.
- Spiegel, M. R. (1965). *Laplace transforms*, Schaum, New York.
- Stehfest, H. (1970). "Numerical inversion of Laplace transforms." *Commun. ACM*, 13(1), 47–49.
- Watson, G. N. (1958). *A treatise on the theory of Bessel functions*, 2nd Ed., Cambridge University Press, Cambridge, U.K.
- Wynn, P. (1956). "On a device for computing the $e_m(S_n)$ transformation." *Math. Tables Aids Comput.*, 10, 91–96.